

# SINGLE $\text{Ca}^+$ ION TRAPPING AND QUADRUPOLE TRANSITION MEASUREMENT TOWARDS AN OPTICAL FREQUENCY STANDARD

Kensuke Matsubara, Ying Li, Hiroyuki Ito, Shigeo Nagano,  
Kazuhiro Hayasaka, and Mizuhiko Hosokawa  
National Institute of Information and Communications Technology  
4-2-1 Nukui-Kitamachi, Koganei, Tokyo 184-8795, Japan  
E-mail: [matubara@nict.go.jp](mailto:matubara@nict.go.jp)

## Abstract

*NICT in Japan is developing an optical frequency standard using a quadrupole transition of single  $\text{Ca}^+$ . After our first measurement, reported at PTTI 2006, we have improved the experimental setup. We have performed laser cooling using two cooling lasers, improved vacuum pressure with an additional getter pump, and introduced a pulse-light sequence to the transition measurement. In consequence, we observed the quadrupole transition with a linewidth of  $\sim 25$  kHz in magnetic fields. The center frequency between the  $|4\ ^2S_{1/2}, m_j=-1/2\rangle - |3\ ^2D_{5/2}, m_j=-3/2\rangle$  and the  $|4\ ^2S_{1/2}, m_j=1/2\rangle - |3\ ^2D_{5/2}, m_j=3/2\rangle$  components was preliminarily estimated to be  $411\ 042\ 129\ 782.5 \pm 1.4$  kHz. The measurement will be improved to obtain better uncertainty.*

## I. INTRODUCTION

The uncertainty of primary frequency standards using Cs atoms reaches  $10^{-15}$  and their inherent limits are being discussed. On the other hand, frequency standards using new atomic and ionic materials are proposed for developing more stable and accurate frequency standards. Several groups have measured frequencies of the ionic forbidden transitions in the optical region to apply them to the clock transitions in frequency standards [1]. We are developing an optical frequency standard using a single  $\text{Ca}^+$  ion. One of its advantages is that all the useful transitions are accessible with the existing laser diodes (LDs) [2].

Partial term diagrams of  $^{40}\text{Ca}^+$  and  $^{43}\text{Ca}^+$  ions are shown in Fig. 1. These ions are laser-cooled with the  $^2S_{1/2} - ^2P_{1/2}$  cooling transition at 397 nm and the  $^2P_{1/2} - ^2D_{3/2}$  repump transition at 866 nm. The lifetime of the  $^2D_{5/2}$  state is  $\sim 1.2$  s (natural linewidth  $\sim 0.2$  Hz), which gives a very high line-Q ( $\sim 10^{15}$ ) to the electric quadrupole  $^2S_{1/2} - ^2D_{5/2}$  transition at 729 nm. An odd isotope like  $^{43}\text{Ca}^+$  ions has the merit that it can avoid the first-order Zeeman frequency shift. We theoretically confirmed that an uncertainty of  $< 1 \times 10^{-15}$  is attainable for  $^{43}\text{Ca}^+$  ions [3]. However, the laser cooling of  $^{43}\text{Ca}^+$  ions requires a much more complicated light source system than  $^{40}\text{Ca}^+$  ions because of the hyperfine splitting. Frequency

measurement of a symmetrical pair of the Zeeman components can average the first-order Zeeman shift in  $^{40}\text{Ca}^+$  ions to zero, and the coefficient of the second-order Zeeman shift in  $^{40}\text{Ca}^+$  ions is much smaller than that in  $^{43}\text{Ca}^+$  ions. Therefore, we are now measuring the  $^2S_{1/2} - ^2D_{5/2}$  transition of  $^{40}\text{Ca}^+$  ions, and in this case we can expect an uncertainty of  $\sim 1 \times 10^{-15}$  [4].

In this paper, we first explain our ion trap and light sources. Then, we explain our spectroscopy after PTTI 2006. Finally, the conclusion and the future plan are described.

## II. ION TRAP AND LIGHT SOURCE SYSTEM

The ion trap and the light source system are almost the same as those reported at PTTI 2006 [5]. Here, we review them briefly and explain some recent improvements. The experimental setup is shown in Fig. 2. A small radio-frequency trap consisting of one ring and two end-cap electrodes is used for the ion trapping. There is a 0.6-mm-radius hole in the ring electrode and the end-cap electrodes are 1.2-mm-diameter rods. A pair of auxiliary rod electrodes, called the “compensation electrode,” is placed near the ring electrode, which compensates the stray electric field. An RF voltage of 300 V at 23 MHz is applied to the ring electrode. This year, we improved the vacuum pressure of the trap chamber using an additional getter pump (SAES) together with an ion pump (Varian). The pressure has been improved from  $\sim 7 \times 10^{-8}$  Pa to  $\sim 1.5 \times 10^{-8}$  Pa. As the result, the collision rate between the trapped ion and the background gases is reduced, and the continuous ion-trapping time period is extended from  $\sim 2$  h to 4~6 h. So we have obtained enough time to optimize the experimental conditions.

For the laser cooling of  $\text{Ca}^+$  ions, we use Littrow-type extended-cavity diode lasers (ECDLs) with an 866-nm LD (Toptica) and a 397-nm LD (Nichia). The frequencies are stabilized with use of a stabilized He-Ne laser (Melles Griot) as the frequency reference [6]. The frequency of the stabilized 866-nm light is measured with an optical frequency comb (Menlo Systems), and the Allan variance is evaluated to be  $< 10^{-10}$  from a 1-s to  $10^3$ -s averaging time. This frequency drifts for  $< 300$  kHz in 2 h. The frequency drift of the stabilized 397-nm light was estimated to be smaller than 2 MHz per hour. They are stable enough to use for the laser cooling of  $\text{Ca}^+$  ions.

Figure 3 shows a highly stable frequency-tunable light source system consisting of a master and slave laser at 729 nm. For the master laser, a Littman-type ECDL with an AR-coated LD (Toptica) is used. To compress its linewidth and frequency drift, the output from the master laser is coupled into a high-finesse ( $F = 6 \times 10^4$ ) ultra-low-expansion (ULE) optical cavity. The frequency of the slave laser is locked to the master laser with a difference of an offset frequency that is provided by a local oscillator. The full width at half maximum (FWHM) of linewidth of the slave laser is  $\sim 66$  Hz. The Allan variance was to be  $< 10^{-12}$  from a 1-s to  $10^2$ -s averaging time. The frequency drift was measured to be  $< 1$  Hz per 1 s.

We produced  $^{40}\text{Ca}^+$  ions from a Ca atomic beam using the photo ionization technique. Neutral Ca atoms are ionized by a two-step photo-excitation at 423 nm and  $< 390$  nm. 423-nm light of  $\sim 100$   $\mu\text{W}$  is produced by the second-harmonic generation with an 846-nm laser diode using a periodically poled (pp) KTP crystal. Light at  $< 390$  nm is obtained from a ultraviolet LD at 375 nm (Nichia).

In addition, 854-nm light is produced from a Littman-type ECDL. It is used to return a  $^{40}\text{Ca}^+$  ion in the meta-stable  $^2D_{5/2}$  state, after the quadrupole transition, into the laser-cooling cycle.

### III. SPECTROSCOPY

#### A. ION LOADING AND MICROMOTION COMPENSATION

We have developed a computer-aided loading system of a single  $^{40}\text{Ca}^+$  ion into the ion trap. In this procedure, a computer program turns on the Ca oven and the photo ionization at the same time for a preset time. Optimizing the oven current (typically 2.1 A) and the preset time (typically 80 s), we can load a single  $\text{Ca}^+$  ion into the trap at a probability of  $\sim 50\%$  of trials. When more than one ion is loaded in the trap, we use another computer program. It blocks incidence of the repump laser at 866 nm for  $\sim 1$  s and decreases the RF voltage amplitude to the ring electrode simultaneously. After running this program two or three times, the number of the trapped ions is decreased to one. A typical counting rate of  $\sim 7000\text{ s}^{-1}$  is observed for a single laser-cooled  $^{40}\text{Ca}^+$  ion. The single ion trapping is confirmed by observing the quantum jump, which is described in subsection B.

If the single ion is not at the trap center, it suffers a driven motion synchronous with the RF electric field of the trap, which is called the “micromotion” [7]. To avoid the micromotion by correcting the displacement from trap center, potentials are applied to the compensation electrodes. This procedure positions the ion at the trap center and prevents the ion from the RF heating. Amplitude of micromotion can be monitored by the RF-photon correlation technique [8]. In our previous experiment, we had executed this technique using a cooling laser that is incident on the trap along only one direction. However, this technique is not so sensitive to the micromotion perpendicular to the propagating direction of the cooling laser beam. Therefore, multiple cooling laser beams are required for more effective compensation. We now compensate the micromotion using two cooling laser beams along different directions. As the result, we can observe very narrow linewidth in the spectrum of a laser-cooled single  $^{40}\text{Ca}^+$  ion, which is shown in Fig. 4.

#### B. QUANTUM JUMP AND QUADRUPOLE TRANSITION MEASUREMENT

After observing the laser cooling as shown in Fig. 4, we fixed 397-nm light frequency at  $\sim 10$  MHz below the resonance peak and we observed continuous fluorescence intensity from a single  $^{40}\text{Ca}^+$  ion. Single-ion trapping is confirmed by the detection of quantum jumps when 729-nm light is incident on the trap, as shown in Fig. 5. The fluorescence is extinguished when the ion is driven to the meta-stable  $^2D_{5/2}$  state by 729-nm light [9]. It returns when the ion decays back to the ground state and then gets into the laser cooling cycle. When there is only one  $^{40}\text{Ca}^+$  ion in the trap, the observed counting rates are clearly classified to two levels, which indicates whether the ion is in the cooling cycle or in the meta-stable  $^2D_{5/2}$  state.

At PTTI 2006, we reported the quadrupole transition spectrum obtained by counting number of the quantum jump observed in a fixed time period. At that time, the observed linewidth was  $\sim 600$  kHz, and it would suffer the power broadening of the 729-nm clock laser. This year, we have introduced a pulse-light sequence control system [10] to obtain the quadrupole transition spectrum effectively. Its sequence is as follows. A photon counting rate of  $> 5000\text{ s}^{-1}$  is observed for a single laser-cooled  $^{40}\text{Ca}^+$  ion. When the computer detects that the ion is in the laser-cooling cycle, the 397-nm, 866-nm, and 854-nm light are blocked, and 729-nm light is incident on the trap for a few ms. Then, using the 397-nm and 866-nm light, the computer checks the photon counting rate so as to determine if a quadrupole transition occurred. If the counting rate is smaller than a preset threshold, the computer recognizes that the quadrupole transition occurred. The threshold is set to a value between the background rate (usually  $< 1000\text{ s}^{-1}$ ), which is counted when the ion is driven to a meta-stable state, and the rate counted when the ion is in the laser-cooling cycle ( $> 5000\text{ s}^{-1}$ ). After checking of the ion status, the ion is returned to the cooling cycle by 854-nm light if it is in the  $^2D_{5/2}$  state, and the computer detects again that the ion is in the laser-cooling cycle. The timetable of a cycle of this interrogation sequence is shown in Fig. 6. After this interrogation cycle is repeated for a preset number of times (10  $\sim$  40), the transition rate is determined,

and then 729-nm light frequency is changed by a step frequency. The quadrupole transition spectra measured in various magnetic fields are shown in Fig. 7. Because the polarization of the 729-nm light was set parallel to the magnet field, only  $\Delta m_j = \pm 1$  Zeeman components were strongly observed. Each Zeeman component consists of a carrier transition and motional sidebands at  $\pm 1.6$  MHz.

### C. CENTER FREQUENCY MEASUREMENT OF THE ZEEMAN COMPONENT

The first-order Zeeman dependence results in the quadrupole  $^2S_{1/2} - ^2D_{5/2}$  transition splitting into 10 Zeeman components. The relative intensities of the components depend on the orientation of the polarization of the 729-nm light, the direction of propagation of the 729-nm light, and the direction of the magnetic field [11]. When the magnetic field is parallel to the direction of the polarization of the linearly polarized 729-nm light, only the  $\Delta m_j = \pm 1$  components are observed.

We observed spectra of the carrier transitions of the  $|4 \ ^2S_{1/2}, m_j = -1/2\rangle - |3 \ ^2D_{5/2}, m_j = -3/2\rangle$  component and the  $|4 \ ^2S_{1/2}, m_j = +1/2\rangle - |3 \ ^2D_{5/2}, m_j = +3/2\rangle$  component. A pair of examples is shown in Fig. 8. The frequency of the 729-nm light was changed with a step frequency of 4 kHz using a double-pass acousto-optic modulator (AOM). At every frequency, the transition rate was determined from 40 interrogation cycles. The pulse-light duration of the 729-nm light was 2 ms. The observed linewidth was  $\sim 25$  kHz. We observed the pair of the carrier transition for 11 times in a magnetic field of  $\sim 410$   $\mu$ T, and we approximated each line profile by the Lorentz function using a nonlinear least square method. The center frequencies and the standard errors of the approximate Lorentz profiles are shown in Fig. 9.

Because the first-order Zeeman dependence of these two carrier transitions in the frequency shift is equal in magnitude and opposite in direction to each other, the center frequency between these two carrier transitions is independent of the magnetic field. We measured the center frequency by recording the AOM offset frequencies and measuring the master 729-nm laser frequency alternatively. To measure the master laser frequency, we used the femtosecond optical frequency comb system reported at PTTI 2006 [5].

The center frequency was calculated with use of the following equation:

$$f = f(\text{master}) + f(\text{slave} - \text{offset}) + \frac{1}{2} (f(\text{AOM offset: } \Delta m_j = -1) + f(\text{AOM offset: } \Delta m_j = +1)),$$

where  $f(\text{master})$  is the absolute frequency of the master 729-nm laser,  $f(\text{slave} - \text{offset})$  is the frequency difference between the master and the slave lasers, and  $f(\text{AOM offset: } \Delta m_j = \pm 1)$  is the AOM offset frequency at peaks of the  $|^2S_{1/2}, m_j = \pm 1/2\rangle - |^2D_{5/2}, m_j = \pm 3/2\rangle$  carrier transitions, respectively. The base frequencies of the femtosecond optical frequency comb and the local oscillators used in this measurement are linked to the International Atomic Time (TAI). The absolute value of  $f(\text{slave} - \text{offset})$  was fixed to 100 MHz. We verified that  $f(\text{slave} - \text{offset})$  and  $f(\text{AOM offset: } \Delta m_j = \pm 1)$  were positive using a high-finesse spectrum analyzer (Coherent) and a high-resolution wavemeter (High finesse). We calculated the center frequency from the 11 pairs of the carrier transition shown in Fig. 9. These carrier transitions were observed within 2 hours, and the master laser frequency was measured before and after the measurements and at a time between measurement No. 7 and No. 8. We observed the frequency drift of the master laser to be 0.19 Hz/s, which was considered in calculation of the center frequency. This drift is due to the long-term cavity-length drift of the ULE cavity. The center frequency for the 11 measurements and their standard errors are shown in Fig. 10. We estimated the mean value of them to be 411 042 129 782. 5 kHz. The standard deviation was  $\pm 1.4$  kHz.

## IV. CONCLUSION

The calcium ion is very attractive for application in optical frequency standards because its  $4 \ ^2S_{1/2} - 3 \ ^2D_{5/2}$  transition, whose natural linewidth is  $\sim 0.2$  Hz, is measurable with existing LDs. By using

LD-based light sources and a small ion trap, we can develop a robust and compact optical frequency standard. After our first quadrupole transition measurement, which was reported at PTTI 2006, we improved our experimental setup. Cooling laser beams that are incident along two directions made it possible to compensate the excess micromotion effectively. An additional getter pump reduced the vacuum pressure to  $\sim 1.5 \times 10^{-8}$  Pa, with the result that the continuous trap time period was increased. By introducing a pulse-light sequence, we measured the quadrupole transition effectively. In consequence, we observed the Zeeman components of the quadrupole transition with linewidth of  $\sim 25$  kHz. We estimated preliminarily the center frequency between the  $|4^2S_{1/2}, m_j = -1/2\rangle - |3^2D_{5/2}, m_j = -3/2\rangle$  and the  $|4^2S_{1/2}, m_j = +1/2\rangle - |3^2D_{5/2}, m_j = +3/2\rangle$  carrier components to be  $411\,042\,129\,782.5 \pm 1.4$  kHz.

The linewidth of  $\sim 25$  kHz seems to suffer from an ambient magnetic field. We will surround the trap chamber with a magnetic shield. Moreover, we will find out the best time relation in our pulse-light sequence in order to reduce the effect of the AC magnetic field caused by east Japan's main electricity. We need to investigate the systematic errors also. We now aim to observe the quadrupole transition with linewidth of  $< 1$  kHz towards a frequency measurement with an uncertainty of  $\sim 10^{-15}$ .

## REFERENCES

- [1] R. Gill, 2005, "Optical frequency standards," **Metrologia**, **42**, S125-S137.
- [2] M. Kajita, K. Matsubara, Y. Li, K. Hayasaka, and M. Hosokawa, 2004, "Preparing single ions in  $m = 0$  states in the Lamb-Dicke regime," **Japanese Journal of Applied Physics**, **43**, 3592-3595.
- [3] M. Kajita, Y. Li, K. Matsubara, K. Hayasaka, and M. Hosokawa, 2005, "Prospect of optical frequency standard based on a  $^{43}\text{Ca}^+$  ion," **Physical Review A****72**, 043404.
- [4] H. S. Margolis, G. P. Barwood, G. Huang, H. A. Klein, S. N. Lea, K. Szymaniec, and P. Gill, 2004, "Hertz-level measurement of the optical clock frequency in a single  $^{88}\text{Sr}^+$  ion," **Science**, **306**, 1355-1358.
- [5] K. Matsubara, Y. Li, K. Fukuda, H. Ito, S. Nagano, M. Kajita, K. Hayasaka, S. Urabe, and M. Hosokawa, 2007, "Quadrupole transition spectrum measurement of single  $\text{Ca}^+$  ions toward optical frequency standard," in Proceedings of 38<sup>th</sup> Precise Time and Time Interval (PTTI) Systems and Applications Meeting, 5-7 December 2006, Reston, Virginia (U.S. Naval Observatory, Washington, D.C.), pp.123-135
- [6] K. Matsubara, S. Uetake, H. Ito, Y. Li, K. Hayasaka, and M. Hosokawa, 2005, "Precise frequency-drift measurement of extended-cavity diode laser stabilized with scanning transfer cavity," **Japanese Journal of Applied Physics**, **44**, 229-230.
- [7] D. J. Berkeland, J. D. Miller, J. C. Bergquist, W. M. Itano, and D. J. Wineland, 1998, "Minimization of ion micromotion in a Paul trap," **Journal of Applied Physics**, **83**, 5025-5033.
- [8] R. Blumel, C. Kappler, W. Quint, H. Walther, 1989, "Chaos and order of laser-cooled ions in a Paul trap," **Physical Review**, **A40**, 808-823.
- [9] H. Dehmelt, 1982, "Mono-ion oscillator as potential ultimate laser frequency standard," **IEEE Transactions on Instrumentation and Measurements**, **IM-31**, 83-87.
- [10] G. P. Barwood, C. S. Edwards, P. Gill, H. A. Klein, and W. R. C. Rowley, 1993, "Observation of the  $5s^2S_{1/2} - 4d^2D_{5/2}$  transition in a single laser-cooled trapped  $\text{Sr}^+$  ion by using an all-solid-state system of lasers," **Optics Letters**, **18**, 732-734.

- [11] R. D. Cowan, 1981, **The Theory of Atomic Structure and Spectra** (California University Press, Berkeley), p. 446.

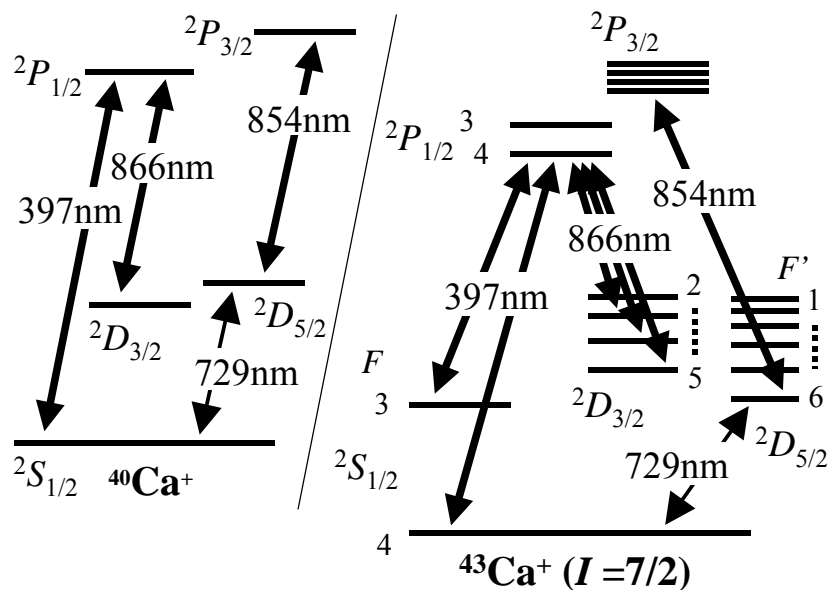


Figure 1. Partial term diagrams of  $^{40}\text{Ca}^+$  and  $^{43}\text{Ca}^+$ .  $F$  and  $F'$  are total angular momentum including nuclear spin  $I=7/2$ .

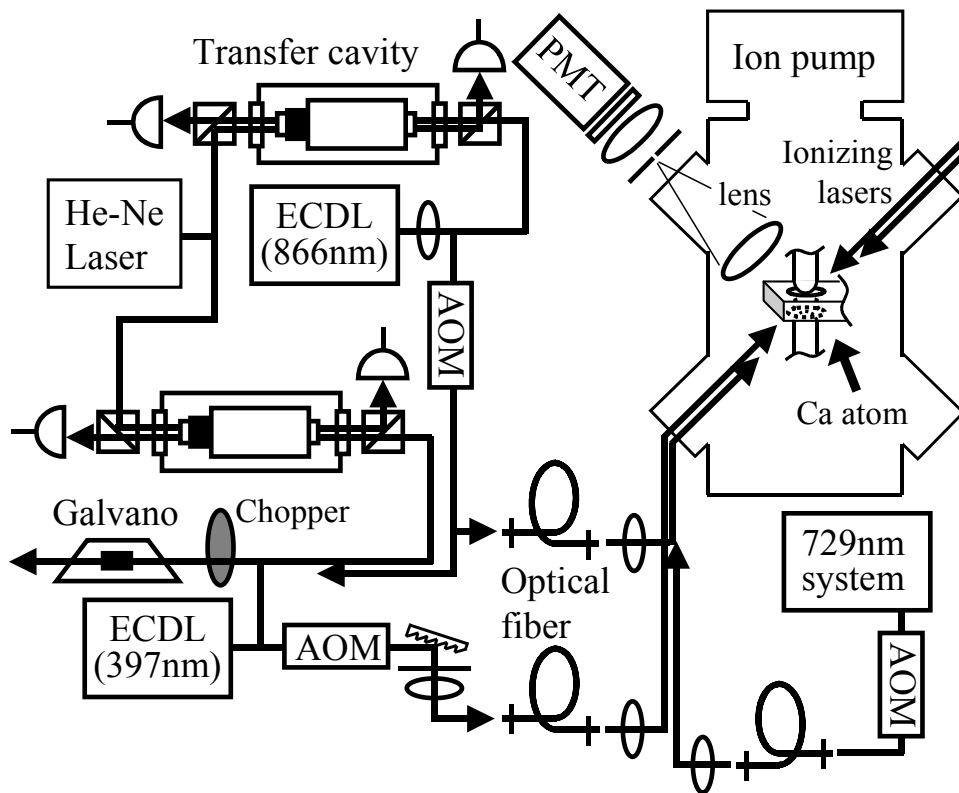


Figure 2. Experimental setup for single  $^{40}\text{Ca}^+$  ions. AOM: acousto-optic modulator; PMT: photo-multiplier tube; Galvano: Galvano tube.

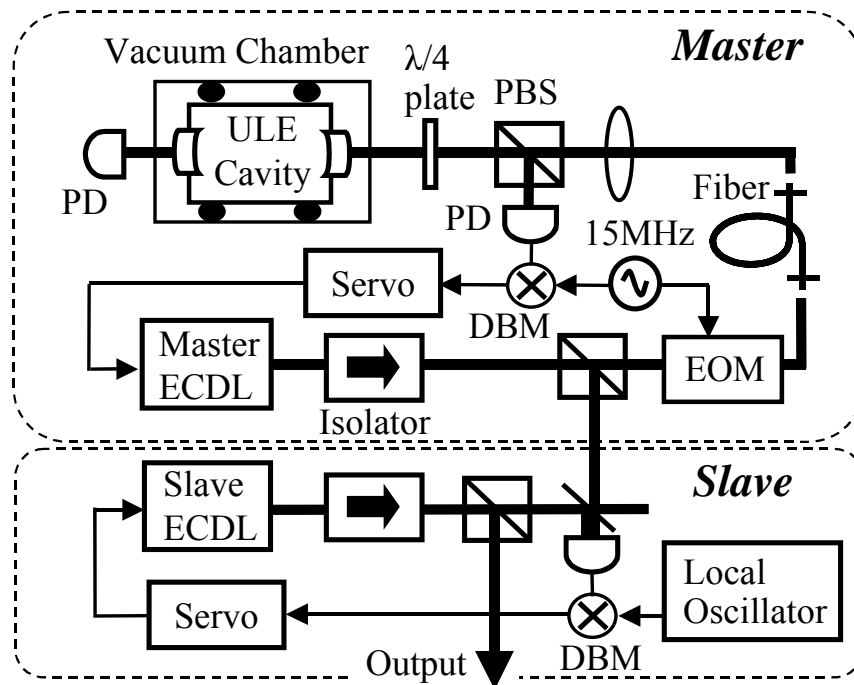


Figure 3. Light source for the quadrupole transition measurement. ULE cavity: ultra-low expansion optical cavity; DBM: double balanced mixer; EOM: electro-optic modulator.

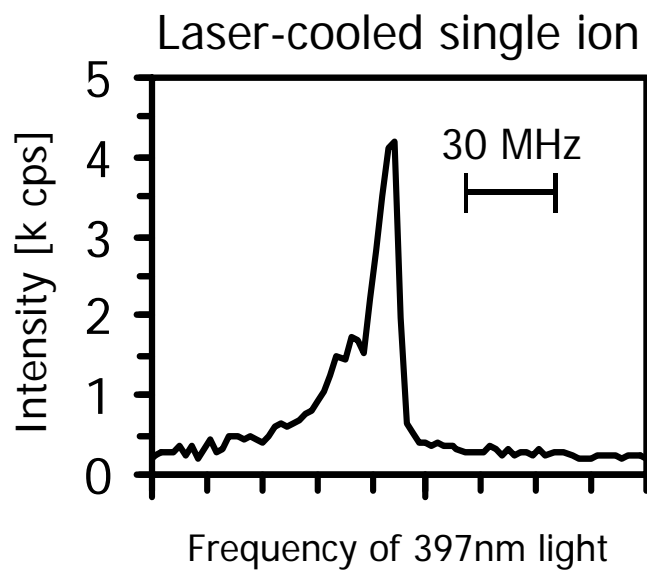


Figure 4. Spectrum of a laser-cooled single  $^{40}\text{Ca}^+$  ion.



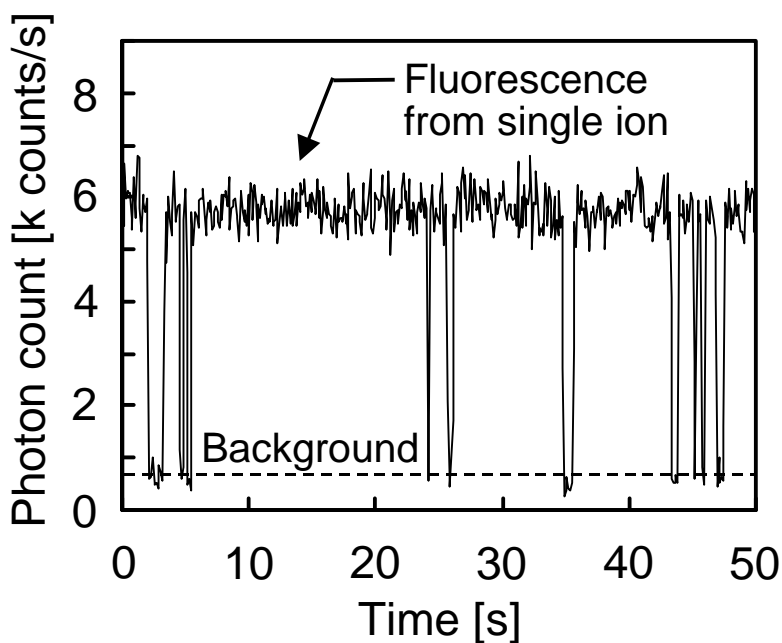


Figure 5. Quantum jumps of a single  $^{40}\text{Ca}^+$  ion.

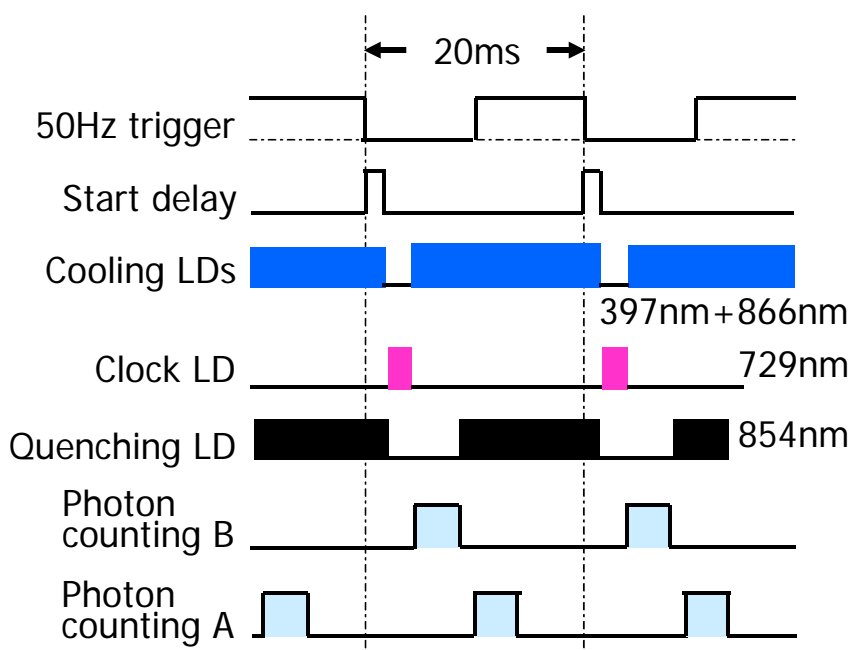


Figure 6. The timetable for the pulse-light sequence. The “counting A” detects that the ion is in the cooling cycle. The “counting B” checks the counting rate to determine if the quadrupole transition occurred. The “50 Hz trigger” synchronizes with east Japan’s main electricity.

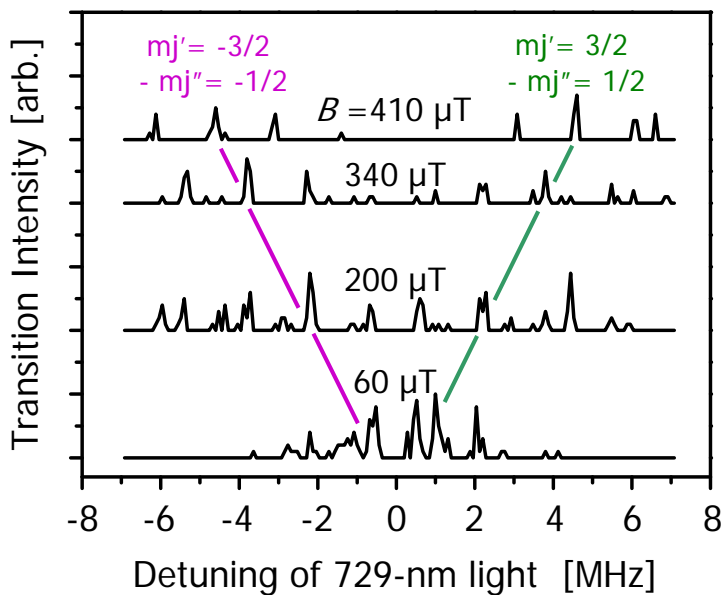


Figure 7. The  $|4 \ ^2S_{1/2}, m_j = \pm 1/2\rangle - |3 \ ^2D_{5/2}, m_j = \pm 3/2\rangle$  components of  $^{40}\text{Ca}^+$ . Polarization of the 729-nm light is parallel to the magnetic field. Red and green lines connect the carrier transitions of each component. The motional sidebands are observed at  $\pm 1.6$  MHz of the carrier transitions.

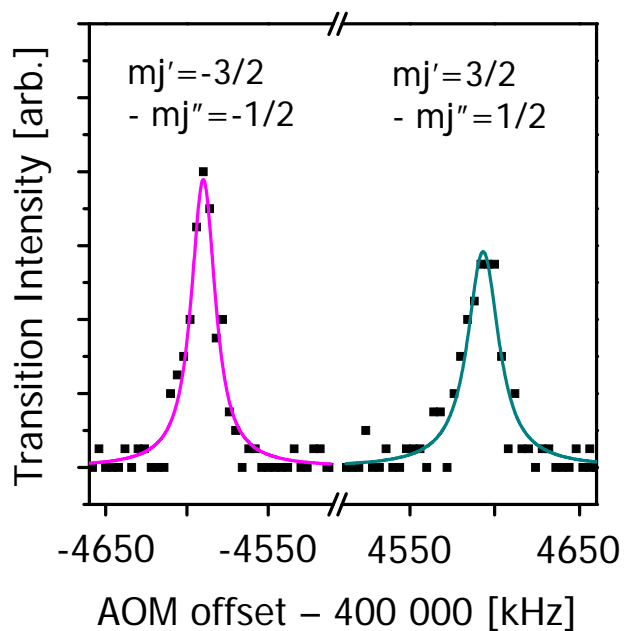


Figure 8. The carrier transitions observed in a magnetic field of  $\sim 410 \ \mu\text{T}$ . They are approximated by the Lorentz functions. The linewidth was estimated to be  $\sim 25$  kHz.

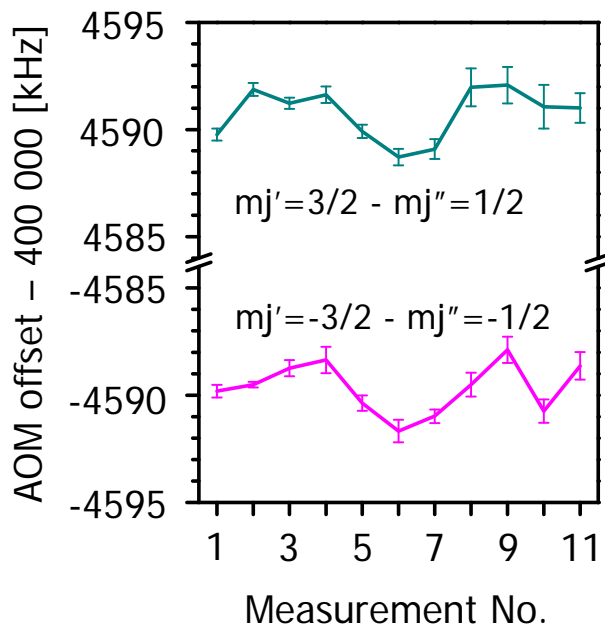


Figure 9. The AOM-offset frequencies at peaks of the approximate Lorenz profiles, and their standard errors. The carrier transitions were observed 11 times in a magnetic field of  $\sim 410 \mu\text{T}$ .

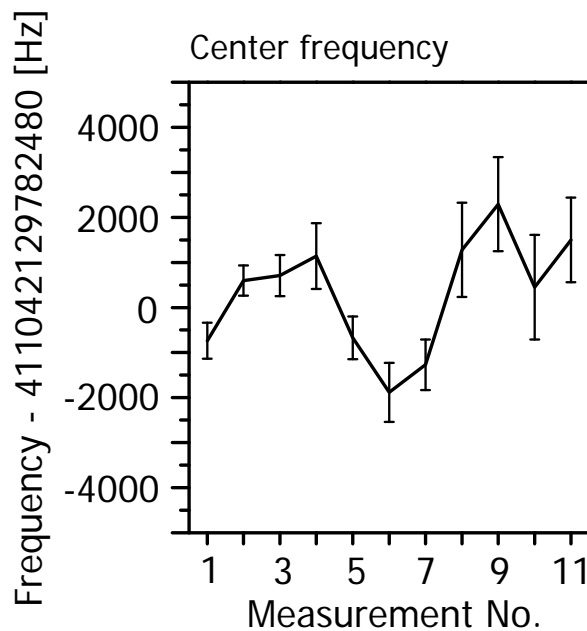


Figure 10. The center frequency between the  $|^2S_{1/2}, m_j = \pm 1/2\rangle - |^2D_{5/2}, m_j = \pm 3/2\rangle$  carrier transitions. The absolute frequency of the master 729-nm laser was measured using an optical frequency comb.

